PERGAMON

Chemical Engineering Science 56 (2001) 5977–5985

Chemical Engineering Science

www.elsevier.com/locate/ces

Analysis of two-phase flow distribution in trickle-bed reactors

A. Souadnia, M. A. Latifi *

Laboratoire des Sciences du Génie Chimique, CNRS-ENSIC, B.P. 451, 1-rue Grandville, 54001 Nancy Cedex, France

Abstract

In the present paper, a phenomenological one-dimensional model of a two-phase gas and liquid flow in a trickle bed reactor is developed. Based on some realistic assumptions specific to tickling flow regime, the original equations of continuity and momentum are reformulated in terms of liquid saturation and gas pressure equations. The computational method used is the finite volume technique combined with Godunov's method. It is shown that the pressure drops derived from the model solution are in good agreement with those measured in the same operating conditions and with previous literature results.

Keywords: Trickle bed reactor; Trickling flow regime; Finite volume method; Godunov's method; Liquid saturation; Gas pressure

1. Introduction

Trickle bed reactors have been widely used in the petroleum industry for many years and are now gaining widespread use in several other fields (Bio-industry, Electrochemical industry, remediation of underground water resources, etc.).

In these reactors whose choice is mainly motivated by hydrodynamic considerations, one or more catalytic reactions (very often liquid/solid) occur. It is therefore evident that the liquid-phase maldistribution is an important factor in the design, scale-up and operation of trickle bed reactors. Packing anisotropy or ineffective liquid inlet distributor may lead to large non-wetted regions of the bed. The main resulting consequences are:

(i) the absence of reactions in the regions of the bed bypassed by the liquid leads to performances (conversion rate, yield, selectivity, etc.) lower than expected. It is worth noticing that the catalyst deactivation may also lower the performances; however, only problems related to liquid-phase maldistribution are considered in this study.

(ii) with no fresh supply of liquid phase which also plays the role of heat carrier, hot-spots may appear for highly exothermic reactions.

It is thus very important to understand the influence of liquid distribution on the reactor performances.

Most of the knowledge about the flow properties of reactors has been obtained through experimental studies; very few works have been devoted to numerical simulations (Biswas & Carey, 1998; Fyhr & Rasmuson, 1996; Jiang, Khadilkar, Al-Dahhan, & Dudukovic, 1999) despite the relevance and increasing interest in modelling and simulation of trickle bed reactors. The contribution of Propp (1998) should be considered among the pioneer works in the area.

The objective of the present paper is, in a first step, to develop a phenomenological model for prediction of pressure drop and liquid flow distribution, and, in a second step, to compare the resulting predictions with experimental measurements in a trickle bed reactor.

The reactor studied here is a packed-bed reactor with co-currently downward gas (nitrogen) and liquid (aqueous caustic soda solutions with hexacyanoferrate II and III ions) flow. It is constituted by a glass column with an inside diameter of 5 cm packed with 5 mm glass spheres. The packing height is 1.6 m and the overall porosity is 0.39 (Naderifar, 1995; Latifi, Naderifar, & Midoux, 1999; Lesage, 2000).

2. Model development

The process considered is a packed bed column where a gas and a liquid flow co-currently downward. The model

* Corresponding author. Tel.: +33-383-1752-34; fax: +33-383-1753-26.

E-mail address: latifi@ensic.inpl-nancy.fr (M. A. Latifi).

0009-2509/01/$ - see front matter
PII: S0009-2509(01)00224-X

developed to describe this multiphase flow is an Eulerian model which consists of continuity and momentum equations of each fluid phase with appropriate closures. In a first step, the model equations are written in their original form using known phenomenological laws. The resulting equations are then reformulated, in a second step, taking into account some simplifying assumptions.

2.1. Original equations

The volume-averaged equations for each flowing phase can be written as

— Continuity equations:

$$\frac{\partial(\varepsilon\rho_i s_i)}{\partial t} + \nabla.(\rho_i u_i) = 0, \quad i = G, L. \tag{1}$$

— Momentum equations:

$$\rho_i \left(\frac{\partial u_i}{\partial t} + u_i \cdot \nabla u_i \right) = \nabla p_i - \rho_i g + F_i + \nabla \cdot (\tau_i + R_i), \quad i = G, L, \tag{2}$$

where F_i denotes the total drag force per unit of bed volume exerted by the phase i, τ_i and R_i are, respectively, the volume averaged viscous stress tensor and the pseudo-turbulence stress tensor of phase i.

— Capillary pressure equation:

$$p_c(s_L) = p_G(s_L) - p_L(s_L). \tag{3}$$

— Saturation sum equation (volume constraint):

$$\sum_i s_i = 1, \quad i = G, L. \tag{4}$$

The resulting model is a system of 6 Eqs. (1–4) in 6 unknowns, i.e. s_L, s_G, u_L, u_G, p_L and p_G. In this paper, instead of solving these original equations, they are reduced to only two equations in two unknowns using some realistic assumptions (Souadnia & Latifi, 2000).

2.2. Equations reformulation

2.2.1. Assumptions

In order to reduce the order of the system (1–4), the following assumptions are introduced:

H1. The flow is in steady state.

H2. Both fluids are incompressible.

H3. The trickling flow regime is considered, i.e. the gas/liquid interactions are low.

H4. The inertial, viscous and pseudo-turbulence terms are neglected compared to the drag force terms.

H5. The porosity is uniform and constant.

H6. The drag forces are accounted for through the following equations developed by Saez and Carbonell (1985):

$$F_i = \frac{\mu_i}{k_{ri}} \left[\frac{A(1-\varepsilon)^2}{d_p^2 \varepsilon^3} + \frac{B\rho_i(1-\varepsilon)|u_i|}{d_p \varepsilon^3 \mu_i} \right] u_i, \quad i = G, L, \tag{5}$$

where A and B are the constants of Ergun's correlation (Ergun, 1952).

H7. The flow is well established in the reactor.

This assumption means that the inertial terms in Eq. (2) are negligible compared to the remaining terms. Eq. (2) are then reduced to a general form of Darcy's law, as follows:

$$u_i = -k_i \left(\frac{k_{ri}}{\mu_i} \right) (\nabla p_i - \rho_i g), \quad i = G, L, \tag{6}$$

where k_i is expressed as

$$k_i = \left(\frac{A(1-\varepsilon)^2}{d_p^2 \varepsilon^3} + \frac{B\rho_i(1-\varepsilon)|u_i|}{d_p \varepsilon^3 \mu_i} \right)^{-1}, \quad i = G, L \tag{7}$$

and k_{ri} are fluid relative permeabilities, given by Saez and Carbonell (1985):

$$k_{rL} = \left(\frac{s_L - s_L^0}{1 - s_L^0} \right)^{2.43} \quad \text{and} \quad k_{rG} = (1 - s_L)^{4.8}, \tag{8}$$

where s_L^0 is the static (residual) liquid hold-up defined by

$$s_L^0 = \frac{1}{\varepsilon(20 + 0.9Eo^*)}. \tag{9}$$

H8. In the trickle bed reactor studied here, the capillary pressure is about 50 Pa whereas the gas pressure is about 1.15×10^5 Pa. In this case, the capillary pressure is negligible and the pressures of gas and liquid phases are assumed to be equal:

$$p = p_L = p_G. \tag{10}$$

However, the gas phase pressure, $p = p_G$, is considered here since the experimental measurements are carried out in the gas phase.

2.2.2. Equations reformulation

Now, by adding the continuity Eq. (1) of each phase and taking into account the volume constraint Eq. (4), the following result is obtained:

$$\nabla \cdot (u_L + u_G) = 0. \tag{11}$$

By replacing the fluid velocities in Eq. (11) by their Eq. (6), the partial differential equation of the gas pressure is derived as

$$\nabla \cdot ((\alpha_L + \alpha_G)\nabla p) = \nabla \cdot (\alpha_L \rho_L + \alpha_G \rho_G), \tag{12}$$

where

$$\alpha_L = k_L\left(\frac{k_{rL}}{\mu_L}\right) \quad \text{and} \quad \alpha_G = k_G\left(\frac{k_{rG}}{\mu_G}\right). \tag{13}$$

On the other hand, by defining the total velocity as

$$u_T = u_L + u_G \tag{14}$$

the use of Eq. (6), leads to

$$u_T = -(\alpha_L + \alpha_G)\nabla p + (\alpha_L\rho_L + \alpha_G\rho_G)g. \tag{15}$$

The liquid velocity in terms of total velocity is then derived as

$$u_L = \frac{\alpha_L}{\alpha_L + \alpha_G}u_T + \frac{\alpha_L\alpha_G}{\alpha_L + \alpha_G}(\rho_L - \rho_G)g. \tag{16}$$

Now, the substitution of Eq. (16) in the continuity equation for liquid Eq. (1) (s_L is easier to measure), allows to obtain:

$$\varepsilon\frac{\partial s_L}{\partial t} + \nabla\cdot\Phi = 0, \tag{17}$$

where the flux Φ is in this case equal to u_L.

The original model equations are thus reduced to two equations: pressure Eq. (12) and saturation Eq. (17). The new model consists then of a parabolic equation (saturation equation) and an elliptic equation (pressure equation).

2.2.3. Important remark

Using the general form of Darcy's law, an implicit non-linearity problem appears in equations reformulation and introduces additional complications to solution computation. This is more illustrated by writing Eq. (6) as

$$u_i = -\alpha_i(s_L, |u_i|)\nabla\hat{p}_i, \quad i = G, L, \tag{18}$$

where $\nabla\hat{p} = \nabla p - \rho g$ and $\alpha_i(s_L, |u_i|)$ means that α_i is a function of s_L and $|u_i|$.

The aforementioned problem becomes evident and is clearly shown since the velocity is involved in both sides of Eq. (18). An explicit expression of velocity is needed in order to solve the problem. To this end, Eq. (7) may be rewritten as

$$k_i = \frac{\mu_i}{Q_i + R_i|u_i|}, \quad i = G, L, \tag{19}$$

where

$$Q_i = \frac{A\mu_i(1-\varepsilon)^2}{d_p^2\varepsilon^3} \quad \text{and} \quad R_i = \frac{B\rho_i(1-\varepsilon)}{d_p^2\varepsilon^3}. \tag{20}$$

The combination of Eqs. (13), (18) and (19) leads to:

$$\alpha_i(Q_i + \alpha_i R_i|\nabla\hat{p}|) = k_{ri}, \quad i = G, L. \tag{21}$$

This second order algebraic equation is solved for $1/\alpha_i$ (α_i being a positive variable) in order to avoid an undefined operation of division whenever R_i or $\nabla\hat{p}$ vanishes during the iteration process. The solution is then given by

$$\alpha_i = \frac{2k_{ri}}{Q_i\left(1 + \sqrt{1 + \dfrac{4k_{ri}}{Q_i^2}R_i|\nabla\hat{p}|}\right)}, \quad i = G, L. \tag{22}$$

The velocity can now be computed explicitly in terms of liquid saturation (through k_{ri}) and gas pressure gradient. The non-linearity problems remaining in s_L and p equations are handled by linearising these equations using a fixed point iteration method (Souadnia & Latifi, 2000).

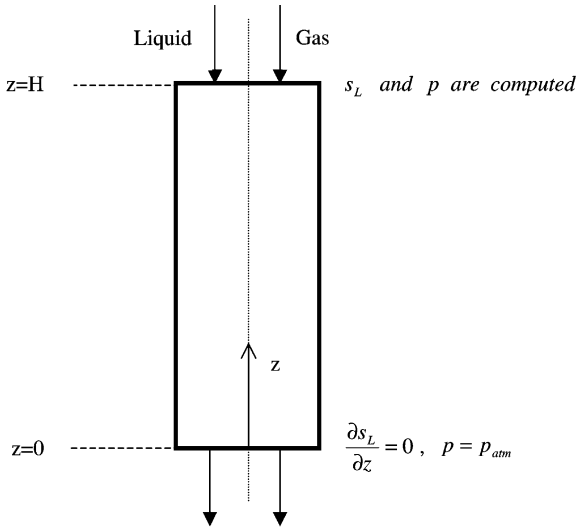

Fig. 1. Reactor scheme and boundary conditions.

2.2.4. Boundary conditions

In this paper, only the one-dimensional model will be considered. Lateral and azimuthal variations of pressure and liquid saturation are therefore assumed to be uniform. Only the axial variations are taken into account. The boundary conditions associated with partial differential Eqs. (12) and (17) are then defined as (Fig. 1):

Packed bed inlet: As we will see later, the computational technique used to solve the model equations is based on finite volume method. Thus, the pressure and liquid saturation at inlet conditions are determined by specifying the gas and liquid velocities (Propp, 1998) as:

— assuming that the liquid is uniformly distributed in the surface area of the top of the reactor, the liquid flowrate at each cell is:

$$u_L^i\Omega^i = -\alpha_L^i\nabla\hat{p}^i\Omega^i, \quad i = 1, 2, \ldots, N, \tag{23}$$

where N is the number of cells, Ω^i the cell cross-sectional area.

— on the other hand, the gas flowrate constraint is given by

$$u_G\Omega = \sum_{i=1}^{N}\alpha_G^i\nabla\hat{p}^i\Omega^i. \tag{24}$$

Relations (23) and (24) constitute a system of $(N+1)$ equations in $(N+1)$ unknowns. Here the unknowns are chosen to be N liquid saturations, s_L^i, and the pressure at the top, p. They are determined by means of a Newton–Raphson method.

Packed bed outlet: The pressure is specified and is equal to the atmospheric pressure:

$$p = p_{\text{atm}}. \tag{25}$$

For the saturation, the following condition is used:

$$\frac{\partial s_L}{\partial z} = 0. \tag{26}$$

3. Computational method

Eqs. (12) and (17) combined with the boundary conditions Eqs. (23–26) are discretised using the finite volume approach introduced by Patankar (1980). Thus in a cell (or control volume) and for the one-dimensional model, the saturation Eq. (12) is discretised using the Crank–Nicholson scheme, as

$$\varepsilon\frac{s_L^{n+1} - s_L^n}{\Delta t} + \frac{\Phi_{i+1/2}^{n+1/2} - \Phi_{i-1/2}^{n+1/2}}{\Delta z} = 0, \tag{27}$$

where $\Phi_{i+1/2}^{n+1/2}$ is the flux at edge $(i+1/2)$ at half time step $(n+1/2)$.

Since the fluxes Φ depend on liquid saturation and total velocity, the latter variables are computed at cell edges at half time steps. The computation algorithm which allows to determine $\Phi_{\text{edge}}^{n+1/2}$ and consequently s_L^{n+1} from s_L^n defined in the centre of the cell is given by:

1. Compute p^n, the pressure at current time, by solving Eq. (12). The total velocity u_T^n is then deduced using Eq. (15).

2. Extrapolation of liquid saturation s_L^n from cell centres at current time to cell edges at half time step $s_{\text{edge}}^{n+1/2}$ using Godunov's method (Propp, 1998; Souadnia & Latifi, 2000).

3. Computation of total velocity at half time step. This is achieved in two stages:

(i) Prediction of the liquid saturation $s_{L,\text{predicted}}^{n+1}$ at next time step by solving the following equation:

$$\varepsilon\frac{s_{L,\text{predicted}}^{n+1} - s_L^n}{\Delta t} + \nabla\cdot\Phi(s_{\text{edge}}^{n+1/2}, u_T^n) = 0. \tag{28}$$

(ii) The predicted saturation is then used to compute p^{n+1} and subsequently u_T^{n+1}. The total velocity at half time step $(n+1/2)$ is estimated as

$$u_T^{n+1/2} = \tfrac{1}{2}(u_T^n + u_T^{n+1}). \tag{29}$$

4. Finally, the liquid saturation s_L^{n+1} at time step $(n+1)$ is deduced from the following equation:

$$\varepsilon\frac{s_L^{n+1} - s_L^n}{\Delta t} + \nabla\cdot\Phi(s_{\text{edge}}^{n+1/2}, u_T^{n+1/2}) = 0. \tag{30}$$

4. Results and discussion

In this section, some numerical results obtained by means of the one-dimensional model developed above are presented. The theoretical pressure drops deduced from the model are then compared to the experimental measurements obtained in the same operating conditions.

4.1. Numerical results

Simulations are carried out for different values of gas and liquid flow rates. The initial liquid saturation in the reactor is assumed to be uniform and equal to 0.15 (static or residual liquid saturation). The number of cells used in this study is equal to 100 and the integration time step is set to 0.001 s.

For example, for gas and liquid flow rates of $G = 0.61\ \text{kg/m}^2/\text{s}$ and $L = 8.06\ \text{kg/m}^2/\text{s}$, the pressure and liquid saturation profiles are determined after 8 and 25 s of simulation time and presented respectively in Figs. 2 and 3.

It can be noticed that for the simulation time of 8 s (Fig. 2) which is less than the liquid residence time in the reactor, the saturation exhibits a propagation front behaviour, hence showing that the numerical problems are correctly handled by means of the computational method used. The pressure profile presents a change in the slope at the same axial position as the saturation.

When the simulation time is about the liquid residence time in the reactor $(=(H/L)\rho_L\varepsilon s_L)$, i.e. 25 s, the saturation becomes uniform and equal to the specified value at the reactor inlet (Fig. 3). The corresponding pressure profile is, as expected, linear throughout the reactor. The slope of this profile will then be used for comparison with experimental measurements carried out at the same gas and liquid flow rates.

4.2. Comparison with experimental measurements

Experimental measurements of pressure drop are carried out in the reactor described in introduction section for different gas and liquid flow rates and for two values of kinematic viscosity (Naderifar, 1995). The traditional parameters ϕ_L and χ_L:

$$\phi_L = \sqrt{\frac{(\frac{\Delta p}{H})_{LG}}{(\frac{\Delta p}{H})_L}} \quad \text{and} \quad \chi_L = \sqrt{\frac{(\frac{\Delta p}{H})_L}{(\frac{\Delta p}{H})_G}} \tag{31}$$

are used for comparison of results.

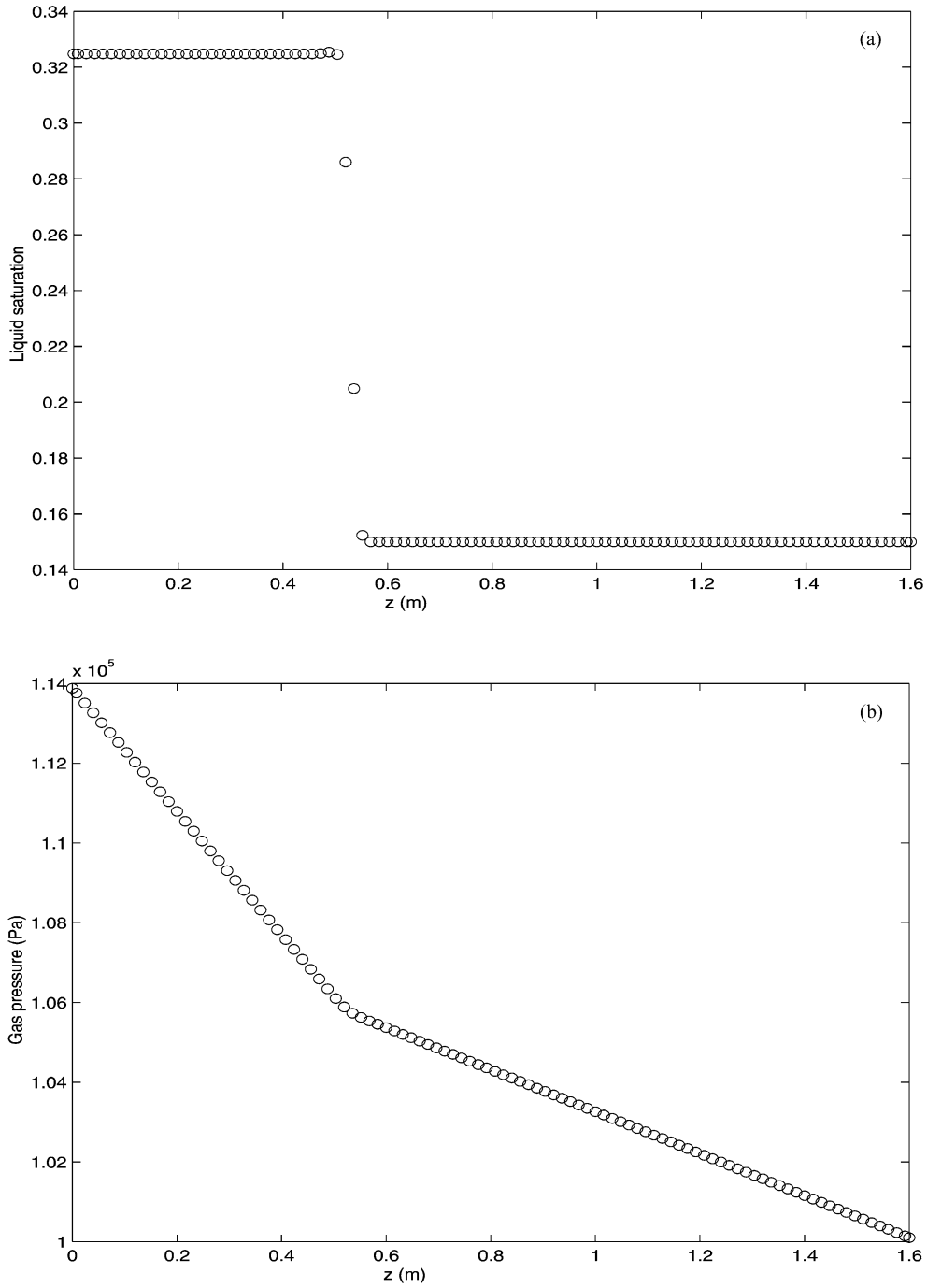

Fig. 2. Simulation results after 8 s of simulation: (a) liquid saturation, (b) gas pressure. $L = 8.06\ \mathrm{kg/m^2/s}$, $G = 0.61\ \mathrm{kg/m^2/s}$, $\mathrm{d}t = 0.001$ s, Number of cells = 100.

Figs. 4 and 5 present in the form of variations of ϕ_L versus χ_L, theoretical and experimental values of pressure drop and the following literature correlations developed by Midoux, Favier, and Charpentier (1976) and Tosun (1984):

$$\phi_L = 1 + \frac{1}{\chi_L} + \frac{1.424}{\chi_L^{0.576}} \quad \text{for } 0.4 \leqslant \chi_L \leqslant 60 \tag{32}$$

and

$$\phi_L = 1 + \frac{1}{\chi_L} + \frac{1.14}{\chi_L^{0.54}} \quad \text{for } 0.1 \leqslant \chi_L \leqslant 80. \tag{33}$$

It can be seen that the agreement between these correlations and both theoretical and experimental results is quite satisfactory. On the other hand, the one-dimensional model developed predicts sufficiently

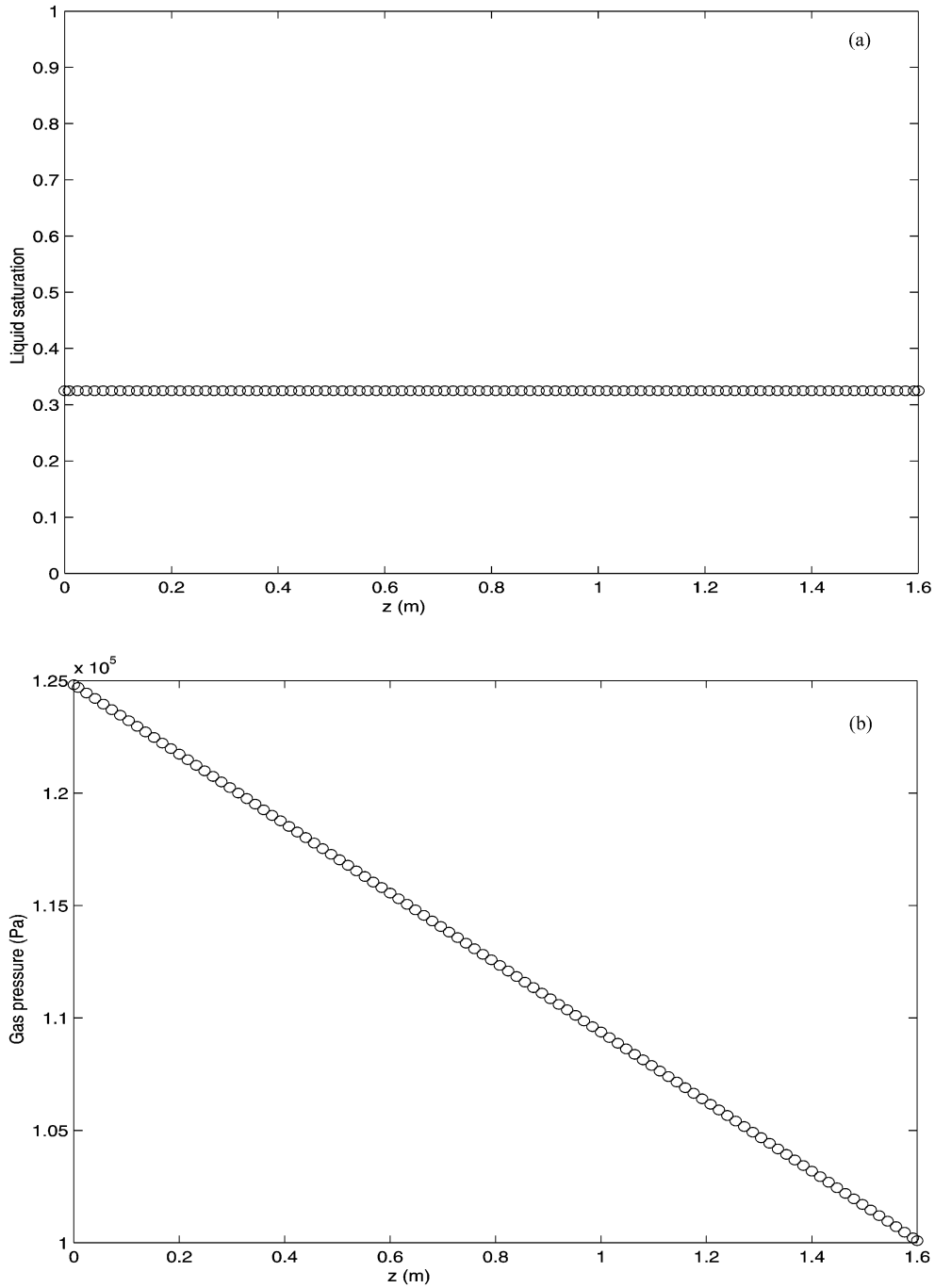

Fig. 3. Simulation results after 25 s of simulation: (a) liquid saturation, (b) gas pressure. $L = 8.06\ \mathrm{kg/m^2/s}$, $G = 0.61\ \mathrm{kg/m^2/s}$, $\mathrm{d}t = 0.001$ s, Number of cells = 100.

well the experimental results. This means that for prediction of overall pressure drops in the trickling flow regime, the 1D model based on the realistic assumptions listed above is appropriate. However, in order to extend the model to pulsing and dispersed flow regimes, further developments are needed. In a first step, a two-dimensional model which takes into account lateral variations of variables should be developed. Then, gas/liquid interactions (Sundaresan, 2000) and eventually porosity profiles should be considered and included in the model.

All these future developments should be based on the direct solution of original equations. Some numerical difficulties encountered in solving the reformulated equations should thus be avoided. Of course, one should be aware of other type of numerical problems that might be posed by the original equations.

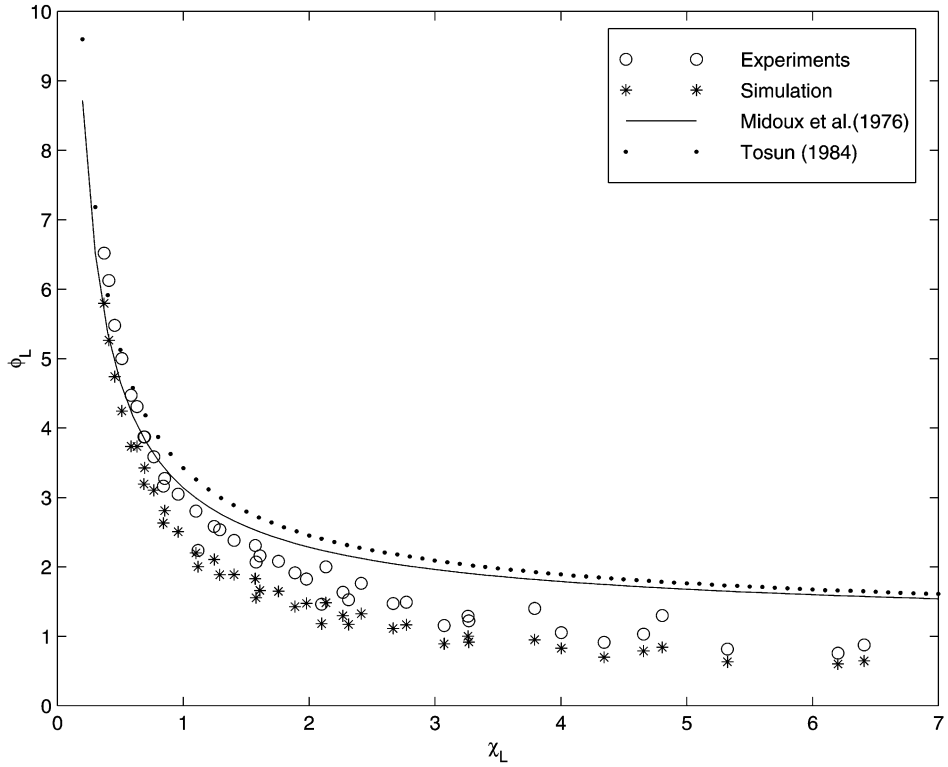

Fig. 4. Comparison of pressure drop results, $v_L = 8.8 \times 10^{-7}$ m^2/s.

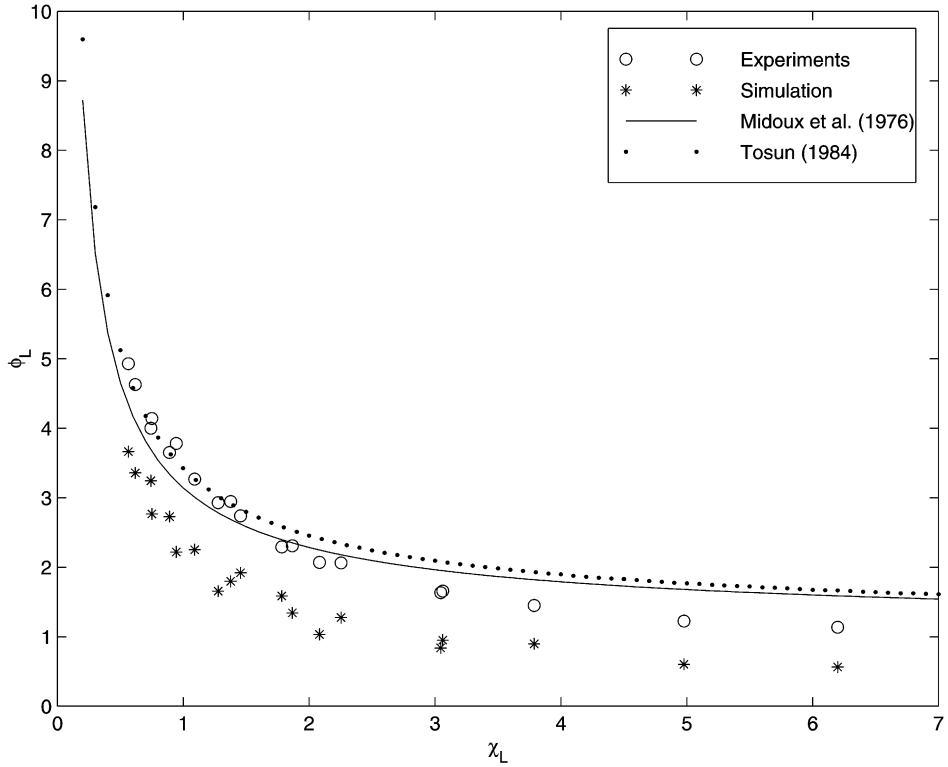

Fig. 5. Comparison of pressure drop results, $v_L = 1.7 \times 10^{-6}$ m^2/s.

The current studies are based on the use of CFDLIB which is a library of multiphase flow codes developed by Los Alamos National Laboratory (Kashiwa, Padial, Rauenzhan, & VanderHeyden, 1994).

5. Conclusions

A one-dimensional model is developed in a trickle bed reactor to predict the liquid saturation and pressure drop in the trickling flow regime, i.e. low gas/liquid interaction regime. The computation method used has shown to be efficient and all numerical problems related to the solution are correctly handled. Moreover, it is shown that pressure drops derived from the model solution are in acceptable agreement with those measured in the same operating conditions.

Among the improvements that are still to be brought to the model in order to better predict the pressure drops and gas and liquid distributions, the development of a two-dimensional model based on the original continuity and momentum equations with appropriate closures. This 2D model will allow to handle momentum transfer in high interaction regimes, i.e. dispersed and pulsing flows. On the other hand, the problem of correlation between gas and liquid pressures is important to investigate and eventually include in the model.

Notation

A 150, coefficient of Ergun correlation
B 1.75, coefficient of Ergun correlation
d_p particle diameter, m
Eo^* modified Eotvos number $= (\rho_L g d_p^2 \varepsilon^2 / \sigma_L (1-\varepsilon)^2)$
H reactor height, m
k permeability, m
k_r relative permeability
p static pressure, Pa
$\hat{p}$ static head pressure, Pa
r radial co-ordinate, m
s saturation
u superficial velocity, m/s
z axial co-ordinate, m

Greek letters

Δp pressure drop, Pa
ε overall bed porosity
μ dynamic viscosity, Pa/s
ν kinematic viscosity, m^2/s
ρ density, kg/m^3
σ surface tension, N/m
ϕ parameter defined in Eq. (31)
χ parameter defined in Eq. (31)
Ω reactor cross-sectional area, m^2

Subscripts

c capillary
G gas phase
L liquid phase
T total

Superscripts

0 static
n current time step

Acknowledgements

The authors are grateful to "Conseil Régional de Lorraine" for financial support of this work.

References

Biswas, D., & Carey, G. F. (1998). A least-squares mixed scheme for the simulation of two-phase flow in porous media on unstructured grids. *Transport in Porous Media*, *32*, 75–95.

Ergun, S. (1952). Fluid flow through packed columns. *Chemical Engineering Progress*, *48*, 88–94.

Fyhr, C., & Rasmuson, A. (1996). Mathematical model of steam drying of wood chips and other hygroscopic porous media. *A.I.Ch.E. Journal*, *42*, 2491–2502.

Jiang, Y., Khadilkar, M. R., Al-Dahhan, M. H., & Dudukovic, M. P. (1999). Two-phase flow distribution in 2D trickle-bed reactors. *Chemical Engineering Science*, *54*, 2409–2419.

Kashiwa, B. A., Padial, N. T., Rauenzhan, R. M., & VanderHeyden, W. B. (1994). A cell-centered ICE method for multiphase flow simulations. *ASME symposium on numerical methods for multiphase flows*, Lake Tahoe, Nevada, USA.

Latifi, M. A., Naderifar, A., & Midoux, N. (1999). Energetic analysis of the liquid-to-wall mass transfer in a trickle-bed reactor. *Transactions of Institution of Chemical Engineers*, *77*(Part A), 69–73.

Lesage, F. (2000). *Modèlisation et expérimentation des phénomènes de transfert de matière et de quantité de mouvement dans les réacteurs à lit fixe*. Ph.D. Thesis, Institut National Polytechnique de Lorraine, Nancy, France.

Midoux, N., Favier, M., & Charpentier, J. C. (1976). Flow pattern, pressure loss and liquid holdup data in gas/liquid downflow packed beds with foaming and non foaming hydrocarbons. *Journal of Chemical Engineering of Japan*, *9*, 350–356.

Naderifar, A. (1995). *Etude expérimentale locale et globale du transfert de matière liquide/solide à la paroi d'un réacteur à lit fixe*. Ph.D. Thesis, Institut National Polytechnique de Lorraine, Nancy, France.

Patankar, S. V. (1980). *Numerical heat transfer and fluid flow*. Washington, DC: Hemisphere publishing corp.

Propp, R. M. (1998). *Numerical modeling of a trickle bed reactor*. Ph.D. Thesis, University of California, Berkley.

Saez, A. E., & Carbonell, R. G. (1985). Hydrodynamic parameters for gas-liquid cocurrent flow in packed beds. *A.I.Ch.E. Journal*, *31*, 52–62.

Sundaresan, S. (2000). Modeling the hydrodynamics of multiphase flow reactors: Current status and challenges. *A.I.Ch.E. Journal*, *46*, 1102–1105.

Souadnia, A., & Latifi, M.A. (2000). Modélisation et simulation des écoulements gaz/liquide dans un réacteur à lit fixe. Research report for "Conseil Régional de Lorraine", LSGC-ENSIC, Nancy, France.

Tosun, G. (1984). A study of cocurrent downflow of nonfoaming gas/liquid systems in a packed bed—2. Pressure drop: Search for a correlation. *Industrial and Engineering Chemistry, Processing Design and Development*, *23*, 35–39.